

1 **Development and Evaluation of Speed Harmonization using Optimal Control Theory:**
2 **A Simulation-Based Case Study at a Speed Reduction Zone**

3 Seongah Hong (corresponding author)
4 Research Assistant
5 University of Virginia
6 351 McCormick Road
7 Charlottesville, VA 22904
8 Tel: 703-965-0244; Email: sh3zm@virginia.edu

9
10 Andreas A. Malikopoulos
11 Deputy Director, Urban Dynamics Institute
12 Energy and Transportation Science Division
13 Oak Ridge National Laboratory
14 Oak Ridge, TN 37831
15 Tel: 865-946-1529; Email: andreas@ornl.gov

16
17 Joyoung Lee
18 Assistant Professor
19 Department of Civil Engineering
20 New Jersey Institute of Technology
21 University Heights
22 Newark, NJ 07102
23 Tel: 434-806-3152; Email: jo.y.lee@njit.edu

24
25 Byungkyu Brian Park
26 Associate Professor
27 Department of Civil and Environmental Engineering
28 University of Virginia
29 P.O. Box 400742
30 Charlottesville, VA 22904-4742
31 Tel: 434-466-9001; Email: bpark@virginia.edu

32
33 Word count: 6,041 words + 5 figures/tables x 250 words (each) = 7,291 words

34 **ABSTRACT**

35 We address the problem of harmonizing the speed of an increasing number of vehicles on a high-
36 way in real time. The objective is to derive the optimal acceleration/deceleration of each vehicle
37 that harmonizes the speed of an increasing number of vehicles at a speed reduction zone on the
38 highway, under the hard safety constraint to avoid rear-end collision. We formulate the control
39 problem and provide an analytical and closed-form solution that can be implemented in real time.
40 The solution yields the optimal acceleration/deceleration of each vehicle under the hard constraint
41 of collision avoidance at the speed reduction zone. The effectiveness of the solution is evaluated
42 through simulation and it is shown that the proposed approach can reduce significantly both fuel
43 consumption and travel time. For different traffic volume levels, the per-vehicle fuel consumption
44 were reduced by 12-17% over the base case and 2-12% over the state-of-the-art VSL algorithm.
45 The travel time was reduced by 28-32% over the base case and 11-28% over the VSL algorithm.

46 *Keywords: Speed harmonization, connected and automated vehicles, traffic flow, optimal control,*
47 *energy usage*

48 I. INTRODUCTION

49 Motivation

50 In a rapidly urbanizing world, we need to make fundamental transformations in how we use and
51 access transportation. This starts with the observation that the purpose of a transportation system
52 is not mobility but rather accessibility to goods, services, and activities. Mobility is only an un-
53 intended outcome of our accessibility needs and may be viewed as an intermediate service (the
54 means) on the way to what we really want: access. As we move to increasingly complex systems
55 (1), new control approaches are needed to optimize the impact on system behavior of the interplay
56 between vehicles at different traffic scenarios.

57 Intersections, merging roadways (2, 3), speed reduction zones along with the drivers' responses to
58 various disturbances (4) are the primary sources of bottlenecks that contribute to traffic congestion
59 (5). In 2015, congestion caused people in urban areas to spend 6.9 billion hours more on the road
60 and to purchase an extra 3.1 billion gallons of fuel, resulting in a total cost estimated at \$160 billion
61 (6). In the US, the average hours annually wasted per commuter was estimated as 50 hours, having
62 ranked the worst country worldwide (7). Particularly, in the most congested metropolitan areas
63 including Los Angeles, CA (81 hours), Washington DC (75 hours) and San Francisco, CA (75
64 hours), in which cities every driver has wasted more than three days in a gridlock traffic a year (7).

65 Speed harmonization is one of the major Intelligent Transportation Systems (ITS) applications op-
66 erated in the US. Instead of having drivers go high speed into a jam, the drivers approach slowly
67 earlier in the upstream, the speed of queue build-up decreases, therefore the congestion recovery
68 time is improved. Eventually, even though their speed may be temporarily reduced, the system
69 is processing vehicles faster. The idea of speed harmonization has been realized through various
70 techniques, such as Variable Message Signs (VMS), Variable Speed Limit (VSL) and the rolling
71 speed harmonization (a.k.a., pace-car technique) (8). Both VMS and VSL systems employ the
72 display gantries mounted along roadways to deliver messages or control schemes. Typical mes-
73 sages provided through VMS systems are road/exit closures, crashes, maintenance/constructions,
74 weather warnings, estimated travel times, etc. While, VSL provides the dynamic speed limits to
75 traffic flow approaching the queues at the downstream bottleneck to reduce the speed variances
76 and mitigate shock waves effects. Another strategy of speed harmonization is so-called the rolling
77 speed harmonization. It uses the designated patrol vehicles entering the traffic to hold a traffic
78 stream to follow them behind at a lowered speed and traverse a congestion area smoothly while
79 mitigating shock waves.

80 Literature Review

81 In the past couple of decades, the practice of speed harmonization has been matured mainly through
82 the VSL strategies which appeared to be more effective and efficient than other techniques such
83 as VMS or the rolling speed harmonization (9, 8). Up to date, advanced VSL strategy employs
84 proactive approach that applies a control scheme beforehand by anticipating the complex behavior
85 of dynamic systems (10). Even though the proactive approach made the VSL systems more ef-
86 fective than ever before, they still remain sub-optimal since they use heuristic approach to search
87 the best solution (11). With an impetus that there was no speed harmonization algorithm which
88 pursues optimal control yet, this study developed a control algorithm or tighten the inflow traffi-
89 cusing the Hamiltonian method through individual vehicular control. Given that the majority of

90 existing VSL strategies rely on macroscopic models which employ aggregated traffic data, consid-
91 ering microscopic behaviors of vehicles to design VSL strategy is expected to improve accuracy
92 in representing traffic conditions, ability to reflect the occurrence of shock waves resulted from the
93 behavior of individual drivers such as sudden deceleration, merging or lane changing (10). Fur-
94 thermore, to provide an environmentally-conscious strategy, our speed harmonization algorithm is
95 designed to minimize acceleration variations which closely relate fuel consumption, while assuring
96 an effective utilization of the roadway and safety elements via explicit constraints within the algo-
97 rithm. In general, minimizing acceleration benefits the fuel consumption since internal combustion
98 engines are optimized over steady state operating points (i.e., constant torque and speed) (12). It is
99 also proven by the fuel consumption model developed by Kamal et al. (13) which demonstrated a
100 monotonic behavior of the fuel consumption with respect to the acceleration, and it becomes even
101 more significant at higher vehicle speeds. The speed harmonization algorithm was evaluated using
102 microscopic traffic simulations under the 100% automated vehicle environment, and the result was
103 compared with one of the state-of-the-art speed harmonization algorithm as well as with no-control
104 case.

105 Speed harmonization strategies can be broadly categorized in reactive and proactive approaches.
106 The reactive approach control initiates the operation at a call upon a queue detected, and it uses
107 immediate traffic condition information to determine a control strategy for the subsequent time in-
108 terval. While the reactive strategy allows to remedy the bottleneck with real-time feedback forward
109 operations, it has limitations related to time lag between the occurrence of congestion and a con-
110 trol implemented (10). In contrast, the proactive approach has the capability of acting proactively,
111 while anticipating the complex behavior of dynamic systems (10). Thus, it can predict bottleneck
112 formations before they even occur. Also, the nature of predictions of proactive VSL strategies
113 allows for more systematic approach for network-wide coordination which supports system opti-
114 mization, whereas reactive approach is restrained to a localized control logic.

115 *Reactive Speed Harmonization*

116 The first field implementation of speed harmonization is known as the VSL system in the German
117 motorway A8 corridor in Munich stretched to the boundary of Salzburg, Austria in 1965 (14). Dur-
118 ing the early 1960s, the US also implemented a VSL with Variable Message Sign (VMS) system
119 on a portion of the New Jersey Turnpike (9). These speed harmonization systems required human
120 interventions to determine the messages or speed limits based on the conditions such as weather,
121 traffic conditions and construction schedules. Since 1970s, advances in sensor technologies and
122 traffic control systems allowed the speed harmonization automatically operated based on the traffic
123 flow or weather conditions using various types of sensors. The earlier VMS and VSL implemen-
124 tations usually address safety issues under work zone areas or inclement weathers (9). In 2007,
125 the speed harmonization strategies aimed at improving traffic flow mobility. The VSL system in
126 the M42 motorway at Birmingham, UK and Washington State Department of Transportation (WS-
127 DOT) (15), the algorithms were automatically activated based on the pre-defined threshold of flow
128 and speed collected from detectors embedded in the pavement and displayed the lowered speed
129 limit within the control zone of pre-defined length (16).

130 Development and evaluations of various VSL algorithms were actively practiced among academic
131 researchers by using simulations tools. The evolution in VSL algorithms that can respond to cur-
132 rent traffic more effectively allowed the performance of VSL to continuously enhance. Park and

133 Yadlapati (17) and Lin et al. (2004) developed reactive approach VSL algorithms to improve
134 safety and mobility at work-zone areas. By determining the VSL control in responsive of the
135 varying travel times in conjunction with the safety surrogate measures, the evaluations showed
136 that the proposed VSL algorithms outperformed the existing VSL algorithms especially with the
137 traffic demand fluctuations thanks to the responsive functions (17). Juan et al. (18) conducted a
138 simulation-based study and concluded that the performance of VSL can vary by the traffic volume
139 levels. After reaching a particular traffic volume level, the benefit can become more apparent, or
140 alternatively less obvious and therefore VSL needs to be intergrated with ramp metering control
141 (18). Kwon et al. (19) developed a VSL algorithm which incorporated the function of identify-
142 ing the moving jam based on the deceleration rate between adjacent spots. With the success in
143 simulation-based evaluations, the VSL algorithm was implemented to the Twin Cities Metropoli-
144 tan areas, MN. The field evaluation showed the reduction in average maximum deceleration by
145 about 20% over the before case and improved the vehicle throughput at the bottleneck areas (19).

146 Through their evolution, the reactive speed harmonization methods have consistently showed im-
147 provements in many aspects such as reliability, safety and environmental sustainability by pro-
148 viding adequate feedback to the dynamic traffic conditions. However, the capability of reactive
149 control is limited as it only responds after a bottleneck occurs and heavily depend on the heuristic
150 approach until the bottleneck is resolved.

151 *Proactive Speed Harmonization*

152 In order to achieve more systematical approach for preventing adverse impacts from impending
153 shock waves, the proactive approach utilizing a prediction model was proposed. The concept
154 of the proactive VSL strategy was first suggested by Alessandri et al. (20). They adopted the
155 Kalman Filter to estimate impending traffic status based on the time-series traffic measurements
156 (21). Given the estimated traffic flow, the VSL control algorithm produced control strategy to
157 minimize various types of cost functions (e.g., average travel time, summation of square densities
158 of all sections) using Powell's optimization method. Although this effort initiated the prediction-
159 based VSL systems, the prediction using a time-series approach is not robust, especially when for
160 unexpected traffic disturbances, since it is heavily relied on the empirical patterns.

161 A pioneering effort in developing a proactive VSL strategy was made by Hegyi et al. (22). They
162 proposed Model Predictive Control (MPC) for the proactive approach VSL systems (22). MPC is
163 a method for the dynamic traffic control problem that optimizes a cost function of the total time
164 spent in the network by all drivers. It performs predictions by explicitly using macroscopic traffic
165 models, and calculates the control scheme that minimizes an objective function. The key element of
166 the Hegyi et al.'s algorithm (22) is that they focused on preventing traffic breakdown by decreasing
167 the density of approaching traffic, rather than focusing on reducing the speed variances. Having
168 the MPC framework which enabled a network-wide optimization, Hegyi et al. (22) coordinated
169 a series of VSLs for the system optimization (22). The idea behind the coordination of multiple
170 VSLs was to resolve shock waves at the bottleneck as well as to prevent having upstream delays
171 (22).

172 Recognizing the capability of MPC method towards handling nonlinear and multi-variable models
173 while providing the capability to consider a network-wide optimization, many researchers adopted
174 MPC to develop proactive VSL methods. Lu et al. (2010) developed a MPC-based proactive VSL

175 algorithm with a different point of view; they focused on creating a discharge section immedi-
176 ate upstream of the bottleneck to regulate traffic flow into the bottleneck and remain close to its
177 capacity. Carlson et al. (23) developed a proactive VSL algorithm aimed at improving solvabil-
178 ity to improve solvability for large-scale network by adopting a discrete-time dynamic optimal
179 control method using the suitable feasible-direction algorithm (24). Furthermore, they applied a
180 rolling horizon mode for providing efficient and simpler feedback control strategies, but their so-
181 lution was sub-optimal (23). The aforementioned MPC-based proactive VSL algorithms showed
182 substantial improvements in vehicle throughput, safety, equity, and driver acceptance under micro-
183 scopic simulation experiments (23, 22, 25, 26). However, these methods impose some challenges
184 in practical applications due to the computational complexity entailed with MPC. According to
185 Frejo and Camacho (11), the average computational time for MPC taken for a unit control horizon
186 was about 316.47 seconds in a Pentium I3 with 3 GHz under the network used in their study. Also,
187 the requirement of model development and calibration is another hurdle that weaken the robustness
188 of their control algorithms.

189 Pursuing a practically applicable algorithm, Hegyi et al. (2008) developed a VSL algorithm so-
190 called, SPECIALIST using shock wave theory. Based on the different traffic states along the
191 freeway segments, their future traffic evolution pattern was predicted. By identifying the location
192 of the front boundaries of shock waves and the active speed limits, VSL control scheme is deter-
193 mined in a way to maximize the discharge rate at the bottleneck (Hegyi et al., 2008). Their control
194 logic is more robust in a way that the model only includes a few parameters that have physical
195 interpretation, such as the maximum thresholds of speed and flow rate at which the traffic status
196 is identified as having shock waves and the speed and the flow associated with free-flow traffic
197 (Hegyi et al., 2008).

198 The performance of the speed harmonization has been varied by control strategies, characteristics
199 of locality and driving behaviors. The travel time improvement has been a debatable point, i.e.,
200 there was no significant change, or even increase in travel time during peak hours (19, 8). However,
201 it has been widely agreed that the speed harmonization helps increase the vehicle throughput at the
202 bottleneck: the vehicle throughput increased by 4-5% via VSL systems (16) and by 5-10 % via
203 rolling speed harmonization implemented in European countries (27). Speed harmonization also
204 benefits the safety; personal injury crashes reduced about 30-35% in European experiments. Crash
205 rate sustained even at the narrowed lanes during construction after the implementation of the VSL.
206 The environmental impacts were substantial as well. Both the practice of VSL and rolling speed
207 harmonization showed reduction in vehicle emissions by 4-10% depending on the pollutants (27),
208 and fuel consumption was reduced by 4% (16).

209 **Organization of the Paper**

210 The structure of the remaining paper is as follows. In Section II we introduce the modeling frame-
211 work, present the assumptions of our approach and formulate the problem. In Section III, we derive
212 a closed-form analytical solution and show that the rear-end collision constraint does not become
213 active. Finally, we provide simulation results in Section IV and concluding remarks in Section V.

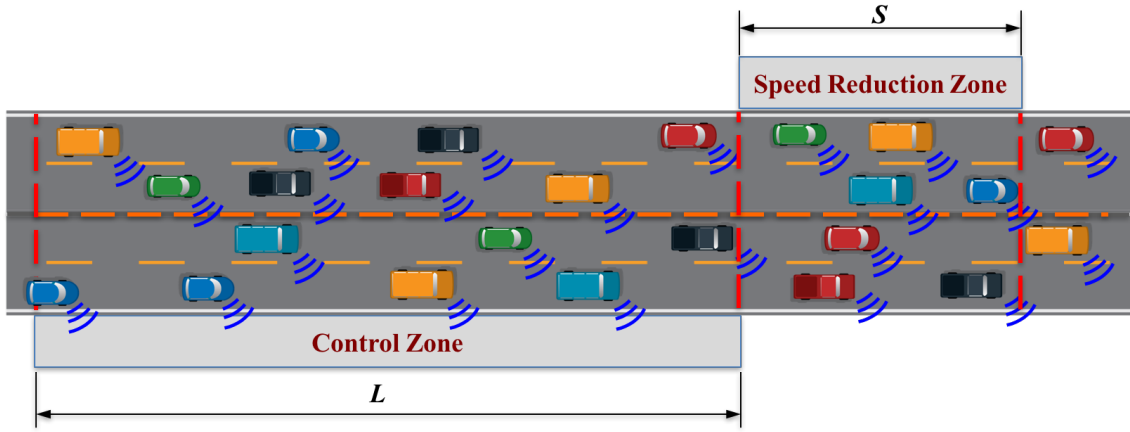


FIGURE 1 Speed harmonization at a speed reduction zone.

214 **II. PROBLEM FORMULATION**

215 We consider a highway with four lanes Figure 1 in each direction and a *speed reduction zone* with
 216 a length S . The highway has a *control zone*, and the distance from the entry of the control zone
 217 until the entry of the speed reduction zone is L .

218 **Modeling Framework**

219 We consider an increasing number of automated vehicles $N(t) \in \mathcal{N}$ in each lane k , $k = 1, \dots, 4$,
 220 where $t \in \mathbb{R}^+$ is the time, entering the control zone. When a vehicle in a lane reaches the control
 221 zone at some instant t , we assign a unique identity $i = N(t) + 1$ which is an integer corresponding
 222 to the location of the vehicle in the queue for each lane k inside the control zone. The number
 223 $N(t)$ can be reset only if no vehicles are inside the control zone. To simplify notation, we restrict
 224 our attention to a single lane.

225 The proposed framework can be extended to multiple lanes, if each vehicle's identity include also
 226 the lane identity. If for example, there is a highway with m lanes, then we can assign an integer
 227 $i = N_k(t) + 1$, where N_k is the number of automated vehicles inside the control zone on the lane
 228 k , $k = 1, \dots, m$.

229 Let $\mathcal{N}(t) = \{1, \dots, N(t)\}$, be the queue in the lane associated with the control zone. We represent
 230 the dynamics of each vehicle $i \in \mathcal{N}(t)$, moving along a specified lane with a state equation

$$\dot{x}_i = f(t, x_i, u_i), \quad x_i(t_i^0) = x_i^0, \quad (1)$$

231 where $t \in \mathbb{R}^+$ is the time, $x_i(t)$, $u_i(t)$ are the state of the vehicle and control input, t_i^0 is the time
 232 that vehicle i enters the control zone, and x_i^0 is the value of the initial state. For simplicity, we
 233 assume that each vehicle is governed by a second order dynamics

$$\begin{aligned} \dot{p}_i &= v_i(t) \\ \dot{v}_i &= u_i(t) \end{aligned} \quad (2)$$

234 where $p_i(t) \in \mathcal{P}_i$, $v_i(t) \in \mathcal{V}_i$, and $u_i(t) \in \mathcal{U}_i$ denote the position, speed and acceleration/deceleration
 235 (control input) of each vehicle i inside the control zone. Let $x_i(t) = [p_i(t) \ v_i(t)]^T$ denote

236 the state of each vehicle i , with initial value $x_i^0 = [0 \ v_i^0]^T$, taking values in the state space
 237 $\mathcal{X}_i = \mathcal{P}_i \times \mathcal{V}_i$. The sets \mathcal{P}_i , \mathcal{V}_i and \mathcal{U}_i , $i \in \mathcal{N}(t)$, are complete and totally bounded subsets of R .
 238 The state space \mathcal{X}_i for each vehicle i is closed with respect to the induced topology on $\mathcal{P}_i \times \mathcal{V}_i$ and
 239 thus, it is compact.

240 We need to ensure that for any initial state (t_i^0, x_i^0) and every admissible control $u(t)$, the system (1)
 241 has a unique solution $x(t)$ on some interval $[t_i^0, t_i^m]$, where t_i^0 is the time that vehicle $i \in \mathcal{N}(t)$ enters
 242 the control zone, and t_i^m is the time that vehicle i enters the speed reduction zone. The following
 243 observations from (2) satisfy some regularity conditions required both on f and admissible controls
 244 $u(t)$ to guarantee local existence and uniqueness of solutions for (2): a) the function f is continuous
 245 in u and continuously differentiable in the state x , b) the first derivative of f in x , f_x , is continuous
 246 in u , and c) the admissible control $u(t)$ is continuous with respect to t .

247 To ensure that the control input and vehicle speed are within a given admissible range, the following
 248 constraints are imposed.

$$\begin{aligned} u_{min} \leq u_i(t) \leq u_{max}, \quad \text{and} \\ 0 \leq v_{min} \leq v_i(t) \leq v_{max}, \quad \forall t \in [t_i^0, t_i^m], \end{aligned} \quad (3)$$

249 where u_{min} , u_{max} are the minimum deceleration and maximum acceleration respectively, and v_{min} ,
 250 v_{max} are the minimum and maximum speed limits, respectively.

251 To ensure the absence of rear-end collision of two consecutive vehicles traveling on the same lane,
 252 the position of the preceding vehicle should be greater than, or equal to the position of the following
 253 vehicle plus a safe distance δ .

254 For each vehicle i , we define the control interval R_i as

$$\begin{aligned} R_i \left\{ u_i(t) \in [u_{min}, u_{max}] \mid p_i(t) \leq p_k(t) - \delta, \right. \\ \left. v_i(t) \in [v_{min}, v_{max}], \forall i \in \mathcal{N}(t), |\mathcal{N}(t)| > 1, \forall t \in [t_i^0, t_i^f] \right\}, \end{aligned} \quad (4)$$

255 where vehicle k is immediately ahead of i on the same road.

256 In the modeling framework described above, we impose the following assumptions:

257 Assumption 1: When the vehicles enter the control zone, the constraints are not active.

258 Assumption 2: For any vehicle $i - 1 \in \mathcal{N}(t)$ traveling on the same road and lane as vehicle
 259 $i \in \mathcal{N}(t)$, $v_{i-1}(t_i^0) \geq v_i(t_i^0) = v_i^0$.

260 Assumption 3: The speed for all vehicles inside the speed reduction zone is v_r , i.e., for all $i \in \mathcal{N}(t)$,
 261 $v_i(t_i^m) = v_i(t_i^f) = v_r$, where t_i^f is the time that each vehicle i exits the speed reduction zone.

262 Assumption 4: Each vehicle i has proximity sensors and can measure local information without
 263 errors or delays.

264 We briefly comment on the above assumptions. The first assumption assures that the solution
 265 will start from a feasible state and control input. The second assumption assures that the rear-
 266 end collision avoidance constraint does not become active at any time in (t_i^0, t_i^m) . The feasibility
 267 enforcement analysis for the vehicles to satisfy such conditions imposed by Assumption 1 is dis-
 268 cussed in (28). The third assumption is a natural consequence of the speed reduction zone since

all vehicles should follow the speed designated in the zone. The fourth assumption might impose barriers in a potential deployment of the proposed framework. However, we could extend our results in the case that this assumption is relaxed, if the noise in the measurements and delays are bounded. In this case, we can determine the uncertainties of the state of the vehicle as a result of sensing and/or communication errors/delays, and account for these in the safety constraints.

Optimal Control Problem Formulation

We consider the problem of minimizing the congestion at the speed reduction zone, shown in Figure 1, with the optimal acceleration/deceleration of each vehicle in terms of fuel consumption under the hard safety constraints to avoid rear-end collision. The potential benefits of the solution of this problem are substantial. By controlling the vehicles in the upstream or tighten the inflow traffic, the speed of queue built-up decreases, and thus the congestion recovery time is also reduced. Even though the speed of each vehicle is reduced, the throughput of the highway is maximized.

When a vehicle enters the control zone, we assign a unique identity as described in the previous section. We formulate $N(t)$ decentralized problems that can be solved in real time. Before we proceed with the decentralized problem formulation we need to establish some definitions.

For each vehicle i when it enters a control zone, we define the *local observation set* $Y_i(t)$ as

$$Y_i(t) \left\{ p_i(t), v_i(t), t_1^m \right\}, \forall t \in [t_i^0, t_i^m], \quad (5)$$

where $p_i(t), v_i(t)$ are the position and speed of vehicle i inside the *control zone*, and t_1^m , is the time targeted for vehicle 1 in the FIFO queue to exit the speed reduction zone. Note that once the vehicle i enters the control zone, then immediately all information in $Y_i(t)$ becomes available to i .

We consider the problem of minimizing the control input at any time for each vehicle from the time t_i^0 it enters the control zone until the time t_i^m that enters the speed reduction zone under the hard safety constraints to avoid rear-end collision. The control problem of coordinating $N(t)$ vehicles in the lane can be formulated as

$$\min \frac{1}{2} \int_{t_i^0}^{t_i^m} u_i^2(t) dt, \quad (6)$$

subject to : (2) and (3),

with boundary conditions $p_i(t_i^0), v_i(t_i^0), p_i(t_i^m)$ and $v_i(t_i^m)$.

III. SOLUTION OF THE OPTIMAL CONTROL PROBLEM

For the analytical solution and real-time implementation of the control problem (6), we apply Hamiltonian analysis. In our analysis, we have assumed (Assumption 3.1) that when the vehicles enter the control zone, none of the constraints are active. However, this might not be in general true. For example, a vehicle may enter the control zone with speed higher than the speed limit. In this case, we need to solve an optimal control problem starting from an infeasible state. The feasibility enforcement analysis for the vehicles to satisfy such initial conditions is discussed in (28).

297 Analytical solution

298 The solution of the problem including the rear-end collision avoidance constraint may become
 299 intractable due to the numerous scenarios of activation/deactivation of the constraints. To address
 300 this problem, the constrained and unconstrained arcs will be pieced together to satisfy the Euler-
 301 Lagrange equations and necessary condition of optimality. Thus, it is not included in the analysis
 302 below. However, we can guarantee rear-end collision avoidance at time t_i^m . In the following
 303 section, we show that the rear-end collision avoidance constraint does not become active at any
 304 time in (t_i^0, t_i^m) assuming it is not active at $t = t_i^0$.

From (6) and the state equations (2), the Hamiltonian function can be formulated for each vehicle $i \in \mathcal{N}(t)$ as follows

$$H_i(t, x(t), u(t)) = L_i(t, x(t), u(t)) + \lambda^T \cdot f_i(t, x(t), u(t)), \quad (7)$$

Thus

$$H_i(t, x(t), u(t)) = \frac{1}{2}u_i^2 + \lambda_i^p \cdot v_i + \lambda_i^v \cdot u_i, \quad (8)$$

305 where λ_i^p and λ_i^v are the co-state components. The necessary condition for optimality is

$$\frac{\partial H_i}{\partial u_i} = u_i + \lambda_i^v = 0, \quad (9)$$

306 From the last equation, the optimal control is given

$$u_i + \lambda_i^v = 0, \quad i \in \mathcal{N}(t). \quad (10)$$

307 The Euler-Lagrange equations yield

$$\dot{\lambda}_i^p = -\frac{\partial H_i}{\partial p_i} = 0 \quad (11)$$

308

$$\dot{\lambda}_i^v = -\frac{\partial H_i}{\partial v_i} = -\lambda_i^p. \quad (12)$$

309 From (11) we have $\lambda_i^p = a_i$ and (12) implies $\lambda_i^v = -(a_i t + b_i)$, where a_i and b_i are constants
 310 of integration corresponding to each vehicle i . Consequently, the optimal control input (accelera-
 311 tion/deceleration) as a function of time is given by

$$u_i^*(t) = a_i t + b_i. \quad (13)$$

312 Substituting the last equation into the vehicle dynamics equations (2) we can find the optimal speed
 313 and position for each vehicle, namely

$$v_i^*(t) = \frac{1}{2}a_i t^2 + b_i t + c_i \quad (14)$$

314

$$p_i^*(t) = \frac{1}{6}a_i t^3 + \frac{1}{2}b_i t^2 + c_i t + d_i, \quad (15)$$

315 where c_i and d_i are constants of integration. These constants can be computed by using the initial
 316 and final conditions. Since we seek to derive the optimal control (13) online, we can designate
 317 initial values $p_i(t_i^0)$ and $v_i(t_i^0)$, and initial time, t_i^0 , to be the current values of the states $p_i(t)$ and
 318 $v_i(t)$ and time t , where $t_i^0 \leq t \leq t_i^f$. Therefore the constants of integration will be functions
 319 of time and states, i.e., $a_i(t, p_i, v_i)$, $b_i(t, p_i, v_i)$, $c_i(t, p_i, v_i)$, and $d_i(t, p_i, v_i)$. To derive online the
 320 optimal control for each vehicle i , we need to update the integration constants at each time t .
 321 Equations (14) and (15), along with the initial and final conditions defined above, can be used to
 322 form a system of four equations of the form $\mathbf{T}_i \mathbf{b}_i = \mathbf{q}_i$, namely

$$\begin{bmatrix} \frac{1}{6}t^3 & \frac{1}{2}t^2 & t & 1 \\ \frac{1}{2}t^2 & t & 1 & 0 \\ \frac{1}{6}(t_i^f)^3 & \frac{1}{2}(t_i^f)^2 & t_i^f & 1 \\ \frac{1}{2}(t_i^f)^2 & t_i^f & 1 & 0 \end{bmatrix} \cdot \begin{bmatrix} a_i \\ b_i \\ c_i \\ d_i \end{bmatrix} = \begin{bmatrix} p_i(t) \\ v_i(t) \\ p_i(t_i^f) \\ v_i(t_i^f) \end{bmatrix}. \quad (16)$$

323 Hence we have

$$\mathbf{b}_i(t, p_i(t), v_i(t)) = (\mathbf{T}_i)^{-1} \cdot \mathbf{q}_i(t, p_i(t), v_i(t)), \quad (17)$$

324 where $\mathbf{b}_i(t, p_i(t), v_i(t))$ contains the four integration constants $a_i(t, p_i, v_i)$, $b_i(t, p_i, v_i)$, $c_i(t, p_i, v_i)$,
 325 $d_i(t, p_i, v_i)$. Thus (13) can be written as

$$u_i^*(t, p_i(t), v_i(t)) = a_i(t, p_i(t), v_i(t))t + b_i(t, p_i(t), v_i(t)). \quad (18)$$

326 Since (16) can be computed online, the controller can yield the optimal control online for each ve-
 327 hicle i , with feedback indirectly provided through the re-calculation of the vector $\mathbf{b}_i(t, p_i(t), v_i(t))$
 328 in (17). Similar results are obtained when the constraints become active as reported in (29).

329 IV. SIMULATION FRAMEWORK AND RESULTS

330 To evaluate the effectiveness of the proposed optimal control algorithm, a simulation framework
 331 was established by integrating a controller and a simulator using the Visual C# programming envi-
 332 ronment. As presented in Figure 2, the optimal control algorithm described in the previous sections
 333 was coded using MATLAB language Dynamic Link Library (DLL) interface programming to al-
 334 low data exchange with other external programs within the framework. A simulation test-bed
 335 network was developed under VISSIM, and it was integrated into the framework by using its COM
 336 interface.

337 The mobility measures such as travel time, average speed and vehicle throughput were directly
 338 obtained from VISSIM. Fuel consumption measure was estimated by using the polynomial meta-
 339 model proposed by Kamal et al. (13) which yielded vehicle fuel consumption as a function of
 340 speed, $v(t)$, and control input, $u(t)$ as in (19).

$$\dot{f}_v = \dot{f}_{cruise} + \dot{f}_{accel} \quad (19)$$

341 where $t \in R^+$ is the time, $\dot{f}_{cruise} = w_0 + w_1 \cdot v(t) + w_2 \cdot v^2(t) + w_3 \cdot v^3(t)$ estimates the fuel
 342 consumed by a vehicle traveling at a constant speed $v(t)$, and $\dot{f}_{accel} = u(t) \cdot (n_0 + n_1 \cdot v(t) + n_2 \cdot v(t)^2)$

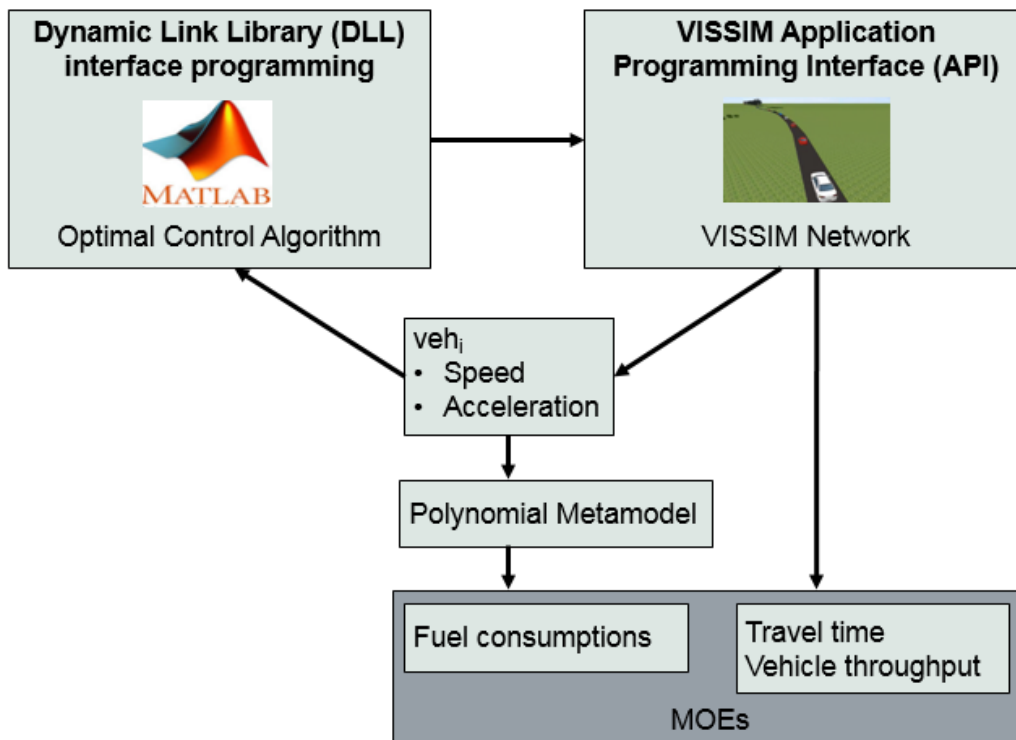


FIGURE 2 Overview of simulation framework

343 is the additional fuel consumption caused by acceleration $u(t)$. The polynomial coefficients w_n ,
 344 $n = 0, \dots, 3$ and r_m , $m = 0, 1, 2$ were calculated from experimental data. For the case studies
 345 we considered in this paper, all vehicles were the same with the parameters reported in (13), where
 346 the vehicle mass was $M_v = 1,200 \text{ kg}$, the drag coefficient was $C_D = 0.32$, the air density was
 347 $\rho_a = 1.184 \text{ km/m}^2$, the frontal area was $A_F = 2.5 \text{ m}^2$, and the rolling resistance coefficient was
 348 $\mu = 0.015$.

349 Test-bed network

350 As noted, the proposed speed harmonization algorithm was implemented in the simulation test-
 351 bed network developed using the VISSIM microscopic traffic simulation program. A hypothetical
 352 test-bed network consists of about 2,000-meter single-lane corridor as shown in Figure 3. A 300-
 353 meter long speed reduction zone which is operated at the speed limit of 35 mph was located at the
 354 downstream of the network and a 300-meter long control zone was created immediate upstream
 355 the entrance of the speed reduction zone, so that the control algorithm effectively applies when
 356 speed deceleration is required.

357 The VISSIM model was carefully calibrated by referring to the guideline of the Highway Capacity
 358 Manual (HCM) 2010 (30). The Chapter 15 of the HCM 2010 (30) presents that the capacity
 359 of two-lane highways under based conditions is 1,700 veh/hr, with a limit of 3,200 veh/hr for
 360 both directions. Without a possibility of having passing maneuvers from the opposite direction
 361 in the proposed test-bed network which is a one-way corridor, a maximum flow rate of 1,800
 362 veh/hr was desired to achieve through calibration. To this end, the key parameters for the car-

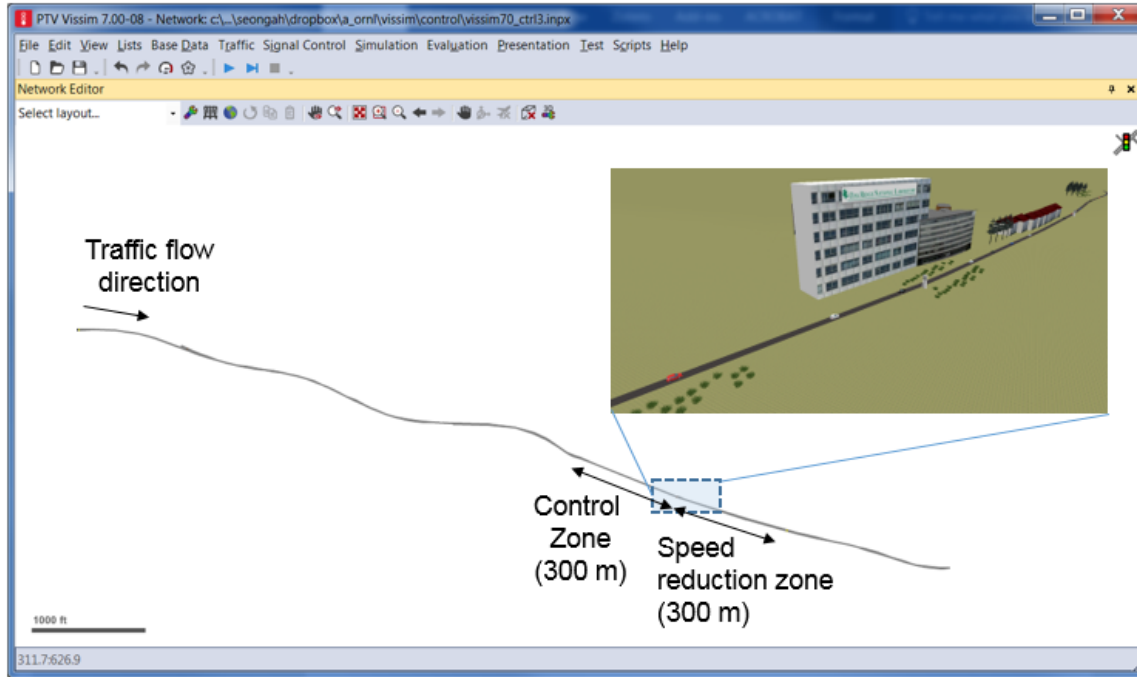


FIGURE 3 Test-bed network developed in VISSIM

363 following model which determine minimum distance between adjacent vehicles were assessed for
 364 calibration. In VISSIM, the minimum safety distance (dx_{safe}) which is defined as a distance a
 365 driver would maintain while following another vehicle can be expressed as shown in (20) (31).

$$dx_{safe} = CC0 + CC1 \cdot v \quad (20)$$

366 where CC0 denotes a standstill distance between two vehicles (in feet), CC1 denotes a headway
 367 time (in seconds) which a driver wants to maintain at a certain speed and v represents average speed
 368 (ft/sec^2). With a good amount of calibration effort, the CC0 was used as the default value of 4.92
 369 feet and the CC1 was adjusted to 1.2 seconds, thereby the maximum traffic flow was approximated
 370 about 1,800 veh/hr as desired.

371 Experimental set-up

372 To assess the impact of the optimal control algorithm under varying traffic volume conditions,
 373 three different volume cases were tested: (i) traffic volume of 1,620 veh/hr which is 10% less than
 374 the capacity (ii) traffic volume of 1,800 veh/hr at the capacity and (iii) traffic volume of 1,980
 375 veh/hr which is 10% more than the capacity. For all scenario cases, the total simulation period was
 376 1,000-second long comprising of 100-second warm-up period and 900-second of control algorithm
 377 implementation to avoid empty network situation during the algorithm applications. 5 replications
 378 of each simulation case were conducted to account for the effect of stochastic components of traffic
 379 and drivers' behaviors, and all produced statistically similar results with a 95% confidence level
 380 (32).

381 The control parameters used for optimal control algorithm are summarized in Table 1. According

TABLE 1 Constraint Parameters of Optimal Control Algorithm

Parameter	Value
Min. speed	10 m/s
Max. speed	35 m/s
Max. acceleration	4.5 m/s^2
Max. deceleration	-4.5 m/s^2
Min. gap distance	20 ft

382 to a guideline published by the Federal Highway Administration (33), the maximum acceleration
 383 and deceleration are suggested as $10ft/sec^2$ (or $3.1m/s^2$) and $-15ft/sec^2$ (or $-4.5m/s^2$), respec-
 384 tively. Considering vehicle technical feasibility of automated vehicles, the maximum acceleration
 385 threshold was relaxed to $15ft/sec^2$ (or $4.5m/s^2$) and the maximum deceleration was adopted as
 386 the guideline taking account for the safety and comfortable driving behaviors. The minimum gap
 387 distance of 20 ft was determined based on the shortest time headway of automated vehicles. Ac-
 388 cording to Gouy et al. (34), the minimum safety headway of automated vehicles was observed as
 389 0.3 seconds under which a vehicle can travel about 20 ft with the maximum speed of 35 m/s^2
 390 in this study. For a constancy between the controller and the traffic simulator, the optimal con-
 391 trol strategy was calculated and updated every 0.1 seconds which is identical with the VISSIM
 392 microscopic simulator resolution.

393 To assess the performance of the optimal control algorithm, two comparison groups were devel-
 394 oped: (i) a base case associated with human drivers based on the Wiedemann 99 psycho-physical
 395 car-following model and (ii) the state-of-the-art VSL algorithm called SPECIALIST (SPEEd Con-
 396 trollIng ALgorIthm using Shock wave Theory) (35). The SPECIALIST algorithm is a proactive
 397 VSL algorithm which projects a traffic conditions in the near future using the Model Predictive
 398 Control (MPC) method (35). The highlight of the SPECIALIST is that the algorithm utilizes the
 399 shock wave theory to generate the control scheme (e.g., control speed and control duration), thus it
 400 does not require complicated computation and only has a few parameters with physical interpreta-
 401 tions that helps for feasible field implementations (35). In this study, the SPECIALIST algorithm
 402 was modeled using the C# programming and implemented in the VISSIM using its COM interface.
 403 Since the SPECIALIST algorithm bases on a mesoscopic model which utilizes the spot-based mea-
 404 surement collected at a fixed location and aggregated for a certain period of time, detector stations
 405 were evenly embedded at every 250 feet along the corridor to estimate the local traffic states. The
 406 traffic state of each detector station was estimated every 60 seconds by using the aggregated esti-
 407 mation of the latest 60-second interval, and the activation of VSL was examined every 60 seconds
 408 as well. Once the control scheme was generated, new measurement was not updated until the cur-
 409 rent control was finished. It is important to mention that the vehicles within the control zone were
 410 ensured to follow the VSL control scheme at 100% compliance rate without perception-reaction
 411 time. Such ideal condition was necessary for a fair comparison with the optimal control algorithm
 412 which assumed 100% automated vehicle environment. The SPECIALIST algorithm had several
 413 parameters that can be selected by the operator. For the best performance of the algorithm, the
 414 parameters were tuned with several iterations. The thresholds of v_{max} and q_{max} were chosen as
 415 35 mph and 1,500 veh/hr, respectively, which were determined after empirical trials to find the
 416 minimum values above which traffic congestion was not observed under the VSL implemented at
 417 the 100% automated vehicle market penetrations. Remaining design parameters (e.g., the shock

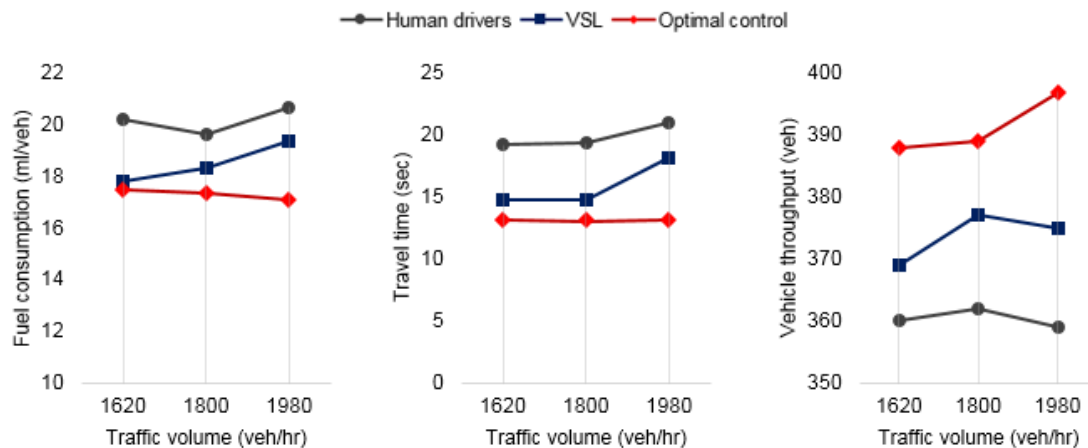


FIGURE 4 Comparisons among Base, VSL and Optimal control

418 wave propagation speed, the density within the zone where VSL is deployed, and the density and
 419 flow after the shock wave is resolved) were adopted from the earlier study (35).

420 Results and analysis

421 Figure 4 presents mobility and fuel economy measures of no-control, the VSL algorithm and the
 422 proposed optimal control algorithm. When compared with no-control and VSL algorithm, the
 423 optimal control algorithm significantly reduced the per-vehicle fuel consumption by 12-17% over
 424 the no-control case and 2-12% over the VSL algorithm for the three traffic volume cases. Both
 425 the VSL algorithm and the optimal control algorithm improved the fuel consumption by ensuring
 426 vehicles to approach the speed reduction zone with less speed variation compared to the no-control
 427 case, but the VSL algorithm could not provide the optimized control scheme as the control scheme
 428 was heuristic solution. On the contrary, the optimal control algorithm provided vehicles in the
 429 control zone with the optimal strategy to approach the speed reduction zone, thereby the per-
 430 vehicle fuel consumption remain constant for all three traffic volume cases.

431 The optimal control algorithm also improved mobility. Travel time and vehicle throughput were
 432 improved for all three cases of traffic volumes over the no-control and the VSL algorithm. It is
 433 interesting to note that the VSL algorithm reduced the travel time when the traffic volume was less
 434 than or at the capacity, but it became less effective when the traffic volume exceeded the capacity.
 435 On the contrary, the optimal control reduced the travel time under the flow rate 10% more than the
 436 capacity, resulting in the travel time improvements of 32-28% over the base case and 11-28% over
 437 the VSL algorithm.

438 V. CONCLUDING REMARKS AND FUTURE RESEARCH

439 In this paper, we considered the problem of harmonizing in real time the speed of an increas-
 440 ing number of vehicles in a highway. We formulated the control problem and used Hamiltonian
 441 analysis to provide an analytical, closed-form solution that can be implemented in real time. The
 442 solution, when it exists, yields the optimal acceleration/deceleration of each vehicle to cross the
 443 speed reduction zone while maximizing the traffic throughput, and under the hard constraint of

444 collision avoidance. The effectiveness of the proposed solution is demonstrated through simula-
445 tion and it is shown that the proposed approach can reduce significantly both fuel consumption and
446 travel time.

447 In our proposed framework, we did not consider lane changing and we assumed that each vehi-
448 cle can measure local information without errors or delays. The assumption of perfect information
449 seems to impose barriers in a potential implementation and deployment of the proposed framework.
450 Although it is relatively straightforward to extend our results in the case that this assumption is re-
451 laxated, future research should investigate the implications of having information with errors and/or
452 delays to the system behavior. Finally, considering lane changing and mixed traffic, e.g., automated
453 vehicles and human-driven vehicles, would eventually aim at addressing the remaining practical
454 consequences of implementing this framework.

455 **ACKNOWLEDGMENTS**

456 This research was supported by the US Department of Energy's SMART Mobility Initiative. This
457 research project was also partially supported by the Global Research Laboratory Program through
458 the National Research Foundation of Korea (NRF) funded by the Ministry of Science, ICT &
459 Future Planning (2013K1A1A2A02078326). These supports are gratefully acknowledged.

460 **REFERENCES**

- 461 [1] Malikopoulos, A. A., A Duality Framework for Stochastic Optimal Control of Complex Sys-
462 tems. *IEEE Transactions on Automatic Control*, Vol. 61, 10, pp. 2756-2765, 2016 (forthcom-
463 ing).
- 464 [2] Rios-Torres, J. and A. A. Malikopoulos, Automated and Cooperative Vehicle Merging at
465 Highway On-Ramps. *IEEE Transactions on Intelligent Transportation Systems*, 2016 (forth-
466 coming).
- 467 [3] Rios-Torres, J. and A. A. Malikopoulos, A Survey on the Coordination of Connected and
468 Automated Vehicles at Intersections and Merging at Highway On-Ramps. *IEEE Transactions*
469 *on Intelligent Transportation Systems*, 2016 (forthcoming).
- 470 [4] Malikopoulos, A. A. and J. P. Aguilar, An Optimization Framework for Driver Feedback
471 Systems. *IEEE Transactions on Intelligent Transportation Systems*, Vol. 14, No. 2, 2013, pp.
472 955–964.
- 473 [5] Margiotta, R. and D. Snyder, *An agency guide on how to establish localized congestion*
474 *mitigation programs*. U.S. Department of Transportation. Federal Highway Administration,
475 2011.
- 476 [6] Schrank, B., B. Eisele, T. Lomax, and J. Bak, *2015 Urban Mobility Scorecard*. Texas A& M
477 Transportation Institute, 2015.
- 478 [7] INRIX Corporation, *INRIX 2015 Traffic Scorecard*, 2016.
- 479 [8] Roberts, M., *I-70 pace cars experiment is working, CDOT says - just not all the time*, 2012.
- 480 [9] Robinson, M., Examples of Variable Speed Limit Applications. Speed Management Work-
481 shop. Transportation Research Board., 2000.
- 482 [10] Khondaker, B. and L. Kattan, Variable speed limit: A microscopic analysis in a connected
483 vehicle environment. *Transportation Research Part C: Emerging Technologies*, Vol. 58, 2015,
484 pp. 146–159.
- 485 [11] Frejo, J. R. D. and E. F. Camacho, Global Versus Local MPC Algorithms in Freeway Traffic
486 Control With Ramp Metering and Variable Speed Limits. *IEEE Transactions on Intelligent*
487 *Transportation Systems*, Vol. 13, No. 4, 2012, pp. 1556–1565.
- 488 [12] Malikopoulos, A. A., P. Y. Papalambros, and D. N. Assanis, Online Identification and
489 Stochastic Control for Autonomous Internal Combustion Engines. *Journal of Dynamic Sys-*
490 *tems, Measurement, and Control*, Vol. 132, No. 2, 2010, pp. 024504–024504.
- 491 [13] Kamal, M. A. S., M. Mukai, J. Murata, and T. Kawabe, Ecological Vehicle Control on Roads
492 With Up-Down Slopes. *IEEE Transactions on Intelligent Transportation Systems*, Vol. 12,
493 No. 3, 2011, pp. 783–794.
- 494 [14] Schick, P., Influence of Traffic Control Systems on Freeway Capacity and Stability of Traffic
495 Flow. *University of Stuttgart*, 2003, p. 20.

- 496 [15] Brinckerhoff, P., T. Farradyne, and J. C. Burgess, *Active Traffic Management Concept of*
497 *Operations*. Washington State Department of Transportation (WSDOT), 2008.
- 498 [16] Mott MacDonald Ltd., *ATM Monitoring and Evaluation 4-Lane Variable Mandatory Speed*
499 *Limits 12 Month Report*. Highways Agency, Bristol UK, 2008.
- 500 [17] Park, B. and S. S. Yadlapati, Development and Testing of Variable Speed Limit Logics At
501 Work Zones Using Simulation. 2003, Washington, DC., 2003.
- 502 [18] Juan, Z., X. Zhang, and H. Yao, Simulation Research and Implemented Effect Analysis of
503 Variable Speed Limits on reeway, 2004, pp. 894–898.
- 504 [19] Kwon, E., C. Park, D. Lau, and B. Kary, Minnesota Variable Speed Limit System: Adaptive
505 Mitigation of Shock Waves for Safety and Efficiency of Traffic Flows. Washington DC., 2011.
- 506 [20] Alessandri, A., A. Di Febbraro, A. Ferrara, and E. Punta, Optimal control of freeways via
507 speed signalling and ramp metering. *Control Engineering Practice*, Vol. 6, No. 6, 1998, pp.
508 771–780.
- 509 [21] Welch, G. and G. Bishop, *An Introduction to Kalman Filter*. SIGGRAPH 2001, ACM, Inc.,
510 Department of Computer Sceience, University of North Carolina at Chapel Hill, 2001.
- 511 [22] Hegyi, A., B. Schutter, and J. Hellendoorn, Optimal coordination of variable speed limits
512 to suppress shock waves. *Transportation Research Record: Journal of the Transportation*
513 *Research Board*, , No. 1852, 2003, pp. 167–174.
- 514 [23] Carlson, R. C., I. Papamichail, M. Papageorgiou, and A. Messmer, Optimal mainstream traf-
515 fic flow control of large-scale motorway networks. *Transportation Research Part C: Emerg-*
516 *ing Technologies*, Vol. 18, No. 2, 2010, pp. 193–212.
- 517 [24] Papageorgiou, M. and M. Marinaki, *A Feasible Direction Algorithm for the Numerical Solu-*
518 *tion of Optimal Control Problems*. Dynamic Systems and Simulation Laboratory, Technical
519 University of Crete, Chania, Greece, 1995.
- 520 [25] Hegyi, A., B. De Schutter, and H. Hellendoorn, Model predictive control for optimal coordi-
521 nation of ramp metering and variable speed limits. *Transportation Research Part C: Emerging*
522 *Technologies*, Vol. 13, No. 3, 2005, pp. 185–209.
- 523 [26] Hegyi, A., B. DeSchutter, and J. Hellendoorn, Optimal Coordination of Variable Speed Limits
524 to Suppress Shock Waves. *IEEE Transactions on Intelligent Transportation Systems*, Vol. 6,
525 No. 1, 2005, pp. 102–112.
- 526 [27] Fuhs, C., *Synthesis of Active Traffic Management Experience in Euripe and the United States*.
527 US Department of Transportation Federal Highway Administration, 2010.
- 528 [28] Zhang, Y., C. G. Cassandras, and A. A. Malikopoulos, Optimal Control of Connected Auto-
529 mated Vehicles at Urban Traffic Intersections: A Feasibility Enforcement Analysis. In *55th*
530 *Conference on Decision and Control*, 2016 (in review).

- 531 [29] Malikopoulos, A. A., C. G. Cassandras, and Y. Zhang, Decentralized Optimal Control for
532 Connected and Automated Vehicles at an Intersection, 2016, - arXiv:1602.03786.
- 533 [30] TRB, *Highway Capacity Manual 2010*. Transportation Research Board., Washington DC.,
534 5th ed., 2010.
- 535 [31] PTV, *PTV VISSIM Traffic Simulation User Manual: Version 7*, 2014.
- 536 [32] VDOT, *Traffic Operations and Safety Analysis Manual (TOSAM) - Version 1.0*, 2015.
- 537 [33] Dowling, R., A. Skabardonis, and V. Alexiadis, *Traffic analysis toolbox volume III: guidelines*
538 *for applying traffic microsimulation modeling software*, 2004.
- 539 [34] Gouy, M., C. Diels, A. Stevens, N. Reed, and G. Burnett, Do drivers reduce their headway to
540 a lead vehicle because of the presence of platoons in traffic? A conformity study conducted
541 within a simulator. *IET Intelligent Transport Systems*, Vol. 7, No. 2, 2013, pp. 230–235.
- 542 [35] Hegyi, A., S. P. Hoogendoorn, M. Schreuder, H. Stoelhorst, and F. Viti, SPECIALIST: A
543 dynamic speed limit control algorithm based on shock wave theory. In *Intelligent Trans-*
544 *portation Systems, 2008. ITSC 2008. 11th International IEEE Conference on*, IEEE, 2008,
545 pp. 827–832.